Testing the standard model in $B \to K^{(*)} l^+ l^-$

Gustavo Burdman
Fermi National Accelerator Laboratory, P. O. Box 500, Batavia, Illinois 60510
(Received 5 June 1995)

We study the potential of $B \to K^{(*)} l^+ l^-$ decays as tests of the standard model. After discussing the reliability of theoretical predictions for the hadronic matrix elements involved, we examine the impact of different new physics scenarios on various observables. We show that the angular information in $B \to K^* l^+ l^-$ together with the dilepton mass distribution can highly constrain new physics. This is particularly true in the large dilepton mass region, where reliable predictions for the hadronic matrix elements can be made with presently available data. As illustrative examples, we compare the standard model predictions with those of two-Higgs-doublet models as well as top-color models, all of which give distinct signals in this region.

PACS number(s): 13.25.Hw, 12.15.Ji, 12.60.Cn, 12.60.Fr

I. INTRODUCTION

Rare decays of B mesons have a great potential as tests of the standard model (SM). Processes involving flavor-changing neutral currents (FCNC's) are of particular interest given that in the SM they can only proceed via one or more loops. This leads to very small rates allowing at the same time for possible contributions from high-energy scales to produce observable effects. For instance, in the SM the top quark gives a very important, and actually dominant, contribution to the process $b \to s\gamma$. Physics beyond the SM, e.g., involving new heavy particles in the loop, could contribute with comparable effects. In fact the observation by CLEO [1] of the inclusive $b \to s\gamma$ transition already constrains the parameter space of many theories [2]. On the other hand, the process $b \to s l^+ l^-$ involves additional information on FCNC's and is an important complement to $b \to s\gamma$ in testing the SM. Although there is still no observation of any of these modes, the experimental situation looks very promising both at e^+e^- [4] as well as hadronic machines [5]. Unlike in $b \to s\gamma$, where there are no reliable ways to calculate the hadronic matrix elements in exclusive modes (e.g., $B \to K^*\gamma$), the corresponding quantities in $B \to K^{(*)} l^+ l^-$ can be safely predicted with the help of heavy quark symmetry [3]. The fact that these exclusive modes can be theoretically clean together with the additional information resulting from a richer kinematics, make these decays very interesting both theoretically as well as experimentally. While $b \to s\gamma$ proceeds via only one operator, the $b \to s l^+ l^-$ processes receive contributions from two additional operators at the weak scale. This will imply that the information on higher-energy scales, encoded in the coefficients of these operators, not only affects the rates but also the shape of the dilepton mass and angular distributions. The use of both the dilepton mass distribution and the lepton angular information is discussed in the context of the inclusive $b \to s l^+ l^-$ decays in [6]. The exclusive modes are discussed in [7] and also in [8], where only the Dalitz plot is considered in various new physics scenarios. The use of the angular information in these modes is proposed in [9].

In this paper we show that the exclusive mode $B \to K^* l^+ l^-$ is a very sensitive test of the SM. The combination of the angular information together with the dilepton mass distribution can be very effective in discriminating among possible new physics scenarios as well as in constraining them. The reason for this lies in the fact that in the SM the lepton asymmetry (see below) is very large at large dilepton masses due to a rather accidental cancellation among the short-distance coefficients. Therefore deviations from the SM produce a very different lepton forward-backward asymmetry, even in cases where the branching ratio and/or the dilepton mass distribution are not markedly different. To illustrate the power of the lepton angular information as SM tests we compare the SM results to two types of extensions of the SM that give typical signals. One of them, represented here by two-Higgs-doublet models (2 HDM's) tends to give lepton asymmetries that are not very different from the SM, even in cases where the rates are. This is due to the fact that these models do not add new operators to the SM operator basis, therefore respecting the chirality structure and only changing the values of short distance coefficients.

In the second example, additional operators contribute and the subsequent modification of the chiral structure in the operator basis is reflected in large modifications of the angular information. To illustrate these type of models we will use a theory that produces FCNC's at the tree level in a manner that is compatible with current phenomenology. Top-color models [10] fit this description because in these type of scenarios, the large mass of the top quark is explained by new gauge interactions that are strong with the third generation, but rather weak with the first two. As a consequence, the first low-energy test of these models is in B decays, with the $B \to K^{(*)} l^+ l^-$ modes the most sensitive. These type of models have potentially large contributions to operators not entering in $b \to s\gamma$ and they tend to give very different branching ratios as well as lepton asymmetries. We also show the

corresponding predictions for the $B \to K l^+ l^-$ decay.

In Sec. II, we summarize the short-distance structure of $b \to s l^+ l^-$. We emphasize the distinction between theories that respect the SM operator basis and those that expand it. This will prove to be relevant when studying the phenomenology of $B \to K^{(*)} l^+ l^-$ decays. In Sec. III, after reviewing the relations predicted by heavy quark symmetry that allow reliable predictions of $B \to K^{(*)} l^+ l^-$ decays in terms of experimental information from other modes, we write down the helicity amplitudes and the angular observables constructed from them. We also compute the $B \to K l^+ l^-$ dilepton mass distribution. In Sec. IV, we show the predictions of the SM, a two-Higgs-doublet extension of it and of top-color models, in order to compare the signals of these different scenarios. We conclude in Sec. V.

II. SHORT-DISTANCE STRUCTURE

In the SM the diagrams contributing to $b \to s l^+ l^-$ processes are shown in Fig. 1. It is convenient to write down an effective theory at low energies by integrating out the heavy degrees of freedom. These are the W boson and top quark inside the loops in Fig. 1. In general, in theories beyond the SM there will be additional contributions. The effective Hamiltonian can be written as an operator product expansion as

$$H_{\rm eff} = \frac{4}{\sqrt{2}} G_F V_{tb}^* V_{ts} \sum_i C_i(\mu) O_i(\mu) \ , \qquad (1)$$

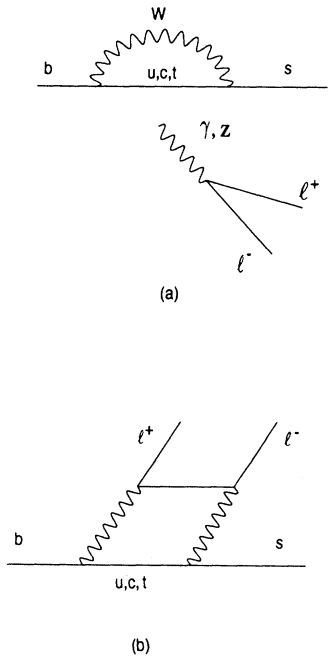

FIG. 1. Diagrams contributing to $b \to s l^+ l^-$.

where $\{O_i(\mu)\}$ is the relevant operator basis and the $C_i(\mu)$ are the corresponding coefficient functions which must cancel the dependence on the energy scale μ. The dimension six operator basis is, in the SM [11,12],

$$\begin{aligned}
O_1 &= (\bar{s}_\alpha \gamma_\mu b_{L\alpha})(\bar{c}_\beta \gamma^\mu c_{L\beta}) \ , \\
O_6 &= (\bar{s}_\alpha \gamma_\mu b_{L\beta}) \sum_q (\bar{q}_\beta \gamma^\mu q_{R\alpha}) \ , \\
O_2 &= (\bar{s}_\alpha \gamma_\mu b_{L\beta})(\bar{c}_\beta \gamma^\mu c_{L\alpha}) \ , \\
O_7 &= \frac{e}{16\pi^2} m_b (\bar{s} \sigma_{\mu\nu} b_R) F^{\mu\nu} \ , \\
O_3 &= (\bar{s}_\alpha \gamma_\mu b_{L\alpha}) \sum_q (\bar{q}_\beta \gamma^\mu q_{L\beta}) \ , \\
O_8 &= \frac{e^2}{16\pi^2} (\bar{s} \gamma_\mu b_L)(\bar{l} \gamma^\mu l) \ , \\
O_4 &= (\bar{s}_\alpha \gamma_\mu b_{L\beta}) \sum_q (\bar{q}_\beta \gamma^\mu q_{L\alpha}) \ , \\
O_9 &= \frac{e^2}{16\pi^2} (\bar{s} \gamma_\mu b_L)(\bar{l} \gamma^\mu \gamma_5 l) \ , \\
O_5 &= (\bar{s}_\alpha \gamma_\mu b_{L\alpha}) \sum_q (\bar{q}_\beta \gamma^\mu q_{R\beta}) \ ,
\end{aligned} \qquad (2)$$

where $q_{L,R} = [(1 \mp \gamma_5)/2] q$ and α, β are color indices. The coefficients at $\mu = m_b$ are obtained when their values at $\mu = M_W$ are evolved using the renormalization-group equation. This has been done in a partial leading logarithmic approximation in [11] for the SM as well as for two-Higgs-doublet models. The complete leading logarithmic approximation for the SM has been recently computed in [13]. For the purpose of this paper it is sufficient to make use of the approximation in [11], given that the uncertainties related to long-distance dynamics, even when reduced by symmetry arguments (see next section), are still larger than the error made by using it. For a complete discussion see [14]. The short-distance information is then encoded in the $C_i(M_W)$'s. Several theories beyond the SM share this operator basis with it. Their extra contributions at the electroweak or higher-energy scales appear as changes in the values of the coefficients at $\mu = M_W$. There are also theories that require an extension of the operator basis. For instance, the chirality of the quark currents could be reversed, giving

$$O_7' = \frac{e}{16\pi^2} m_b (\bar{s} \sigma_{\mu\nu} b_L) F^{\mu\nu} \ , \qquad (3a)$$

$$O_8' = \frac{e^2}{16\pi^2} (\bar{s} \gamma_\mu b_R)(\bar{l} \gamma^\mu l) \ , \qquad (3b)$$

$$O_9' = \frac{e^2}{16\pi^2} (\bar{s} \gamma_\mu b_R)(\bar{l} \gamma^\mu \gamma_5 l) \ , \qquad (3c)$$

as well as the ones resulting from $b_L \to b_R$ in $O_1 - O_6$.

The SM, supersymmetry, multi-Higgs-doublet models and most technicolor scenarios only modify the value of the short-distance coefficients $C_i(M_W)$, without inducing additional operators. On the other hand, left-right sym-

metric models, compositeness, and top-color are among the theories capable of inducing sizable wrong-chirality contributions as well as shifts in the normal-chirality coefficients. These two very different groups of electroweak symmetry breaking scenarios are likely to give drastically different signals, for instance for the angular distributions. The only operator entering in $b \to s\gamma$ at the weak scale is O_7. Therefore, radiative processes have a rather limited power as SM tests: only the shifts induced in $C_7(M_W)$ are probed. Conversely, $b \to sl^+l^-$ processes are more sensitive to new physics which might give small or null deviations of the $b \to s\gamma$ rate but still give large contributions to the other coefficients in (1). These would produce not only a different rate but also distinct patterns in the dilepton mass distributions as well as the angular distributions.

III. RELIABLE PREDICTIONS FOR $B \to K^{(*)}l^+l^-$

The use of experimental information in $b \to sl^+l^-$ processes requires the theoretical understanding of hadronic effects. The inclusive rate $B \to X_s l^+l^-$ is theoretically clean in this respect and can be predicted with rather low uncertainties [6,16]. However, its experimental observation might prove to be a very difficult task. On the other hand, exclusive modes like $B \to Kl^+l^-$ and $B \to K^*l^+l^-$ are more accessible to both e^+e^- and hadronic machines, but the need to compute hadronic matrix elements of the operators in (2) and (3) introduces potentially large hadronic uncertainties. The situation appears to be similar to the one in $B \to K^*\gamma$, where the large disagreement among model calculations of the matrix element of O_7 between B and K^* renders this mode almost useless as a test of the SM. However, in the present case these large uncertainties can be avoided by making use of heavy quark symmetry (HQS), which relates the hadronic matrix elements entering in $B \to K^{(*)}l^+l^-$ decays to those entering in semileptonic decays [3]. It must be emphasized that we *do not* consider the limit in which the s quark is heavy, as is done in part of previous work on these decays. In the rest of this section we review the implementation of these relations and make use of them in $b \to sl^+l^-$ exclusive decays.

A. $B \to K^*l^+l^-$

As we will see below, this mode is the most interesting one from the phenomenological point of view. We need the matrix elements of the operators O_7, O_8, O_9, O_7', O_8', and O_9'. The hadronic matrix elements of O_7 ad O_7' can be written as

$$\begin{aligned}\langle K^*(k)|\bar{s}\sigma_{\mu\nu}(1\pm\gamma_5)b|B(P)\rangle = \epsilon_{\mu\nu\alpha\beta}\{A\epsilon^{*\alpha}P^\beta + B\epsilon^{*\alpha}k^\beta + C\epsilon^*\cdot PP^\alpha k^\beta\} \\ \pm i\{A(\epsilon^{*\mu}P^\nu - \epsilon^{*\nu}P^\mu) + B(\epsilon^{*\mu}k^\nu - \epsilon^{*\nu}k^\mu) \\ + Ce^*\cdot P(P^\mu k^\nu - P\nu k^\nu)\}\ ,\end{aligned} \tag{4}$$

where A, B, and C are unknown functions of $q^2 = (P-k)^2$, the squared momentum transferred to the leptons. On the other hand, the matrix elements of the semileptonic operators O_8, O_9, O_8', and O_9' are parametrized by

$$\langle K^*(k)|\bar{s}\gamma_\mu(1\pm\gamma_5)b|B(P)\rangle = ig\epsilon_{\mu\nu\alpha\beta}\epsilon^{*\nu}(P+k)^\alpha(P-k)^\beta \pm f\epsilon_\mu^* \pm a_+e^*\cdot P(P+k)_\mu \pm a_-e^*\cdot P(P-k)_\mu \tag{5}$$

with g, f, and $a_\pm$ also unknown functions of q^2.

In the heavy quark limit, where the mass of the b quark is infinitely heavy compared to the typical scale of the strong interactions, the Dirac structure of (4) is related to that of (5). The simplification arises because in the $m_b \gg \Lambda_{\rm QCD}$ limit the heavy quark spinor loses its two lower components becoming

$$b(x) \approx \begin{pmatrix} \Psi(x) \\ 0 \end{pmatrix}\ . \tag{6}$$

That is, the two lower components are suppressed by m_b. As a consequence, the action of γ matrices on the b spinor simplifies. One has, for instance, $\gamma_0 b = b$. The $(0i)$ component of (4) is now related to the (i) component of (5) by the relations

$$\begin{aligned} i\sigma_{0i} &= \gamma_i\ , \\ i\sigma_{0i}\gamma_5 &= -\gamma_i\gamma_5\ . \end{aligned} \tag{7}$$

By making use of (7) we can obtain now relations among the form factors in (4) and (5). They are [3]

$$A = \frac{-f + 2m_B k_0 g}{m_B}\ , \tag{8a}$$

$$B = -2m_B g\ , \tag{8b}$$

$$C = \frac{a_+ - a_- + 2g}{m_B}\ . \tag{8c}$$

Furthermore, the semileptonic $B \to K^*$ from factors g, f, and $a_\pm$ are identical to the $B \to \rho l\nu$ form factors in the SU(3) limit. Therefore, the hadronic matrix elements entering in $B \to K^* l^+ l^-$ are given by the $B \to \rho l\nu$ form factors to leading order in $\Lambda_{\rm QCD}/m_b$ and in the SU(3) limit. In this way, experimental information on $B \to \rho l\nu$ can be used as a prediction for $B \to K^* l^+ l^-$. Relations (8) can be also used to predict the $B \to K^*\gamma$ rate. In this case, however, the region of the $B \to \rho l\nu$ Dalitz plot that can be used is negligibly small. This is due to the fact that one needs the semileptonic form factors evaluated at $q^2 = 0$ in the case with a real photon. Moreover, the ρ must be left handed in order to have the same combination of form factors that appear in the radiative decay. Both conditions can only be satisfied in one corner, corresponding to the ρ and the charged lepton having both maximum momenta. The rate at this point vanishes due to phase space, and thus an extrapolation to this point must be made in order to extract a model-independent quantity that would constitute the $B \to K^*\gamma$ hadronic matrix element [17]. The situation is very different here. We are able to use all the $B \to \rho l\nu$ Dalitz plot, which in the SU(3) limit covers exactly the $B \to K^* l^+ l^-$ Dalitz plot.

Presently, there are only upper limits for $B \to \rho l\nu$ [18]. However the observation of $B \to \pi l\nu$ at CLEO [18] indicates that there will be data on this mode very soon. We can make use of present data by taking an extra step in using the heavy quark symmetries. This time we use the flavor symmetry that relates processes with b and c quark hadrons. This implies relations among the semileptonic $B \to K^*$ form factors entering in (5) and those in the decay $D \to K^* l\nu$. Up to a short-distance correction factor, these relations are the simple mass scaling laws [3]:

$$f^B(v\cdot k) = \sqrt{\frac{m_B}{m_D}} f^D(v\cdot k) \ , \tag{9a}$$

$$g^B(v\cdot k) = \sqrt{\frac{m_D}{m_B}} g^D(v\cdot k) \ , \tag{9b}$$

$$(a_+ - a_-)^B(v\cdot k) = \sqrt{\frac{m_D}{m_B}} (a_+ - a_-)^D(v\cdot k) \ , \tag{9c}$$

where the form factors on the left-hand side of (9) are those in $B \to K^* l^+ l^-$ and those on the right-hand side those entering in $D \to K^* l\nu$. Relations (9) are valid when the form factors are evaluated at the same value of $v\cdot k$, with v the heavy meson four-velocity and k_μ the K^* four-momentum. In the rest frame of the heavy meson this is the K^* recoil energy, E_{K^*}. Thus, we can only predict $B \to K^* l^+ l^-$ for values of E_{K^*} ranging from m_{K^*} to the maximum recoil in $D \to K^* l\nu$. In terms of $q^2 = m_{ll}^2$, the dilepton invariant mass squared, this implies the window $4.0 < m_{ll} < 4.4$ GeV, where the upper value is actually the maximum allowed dilepton mass. Model-independent predictions for the $B \to K^* l^+ l^-$ form factors for smaller dilepton masses will only be possible when the $B \to \rho l\nu$ data are available. We will make use of the form factors extracted in $D \to K^* l\nu$ decays [19] to illustrate how the SM predictions compare with those of some of its extensions.

In order to take full advantage of the information provided by this decay we first notice that the amplitude can be divided into two noninterfering pieces corresponding to left- and right-handed leptons. Each of them can then be expressed as a sum of helicity amplitudes. The squared amplitude is

$$|A(B \to K^* l^+ l^-)|^2 = |H_+^L|^2 + |H_-^L|^2 + |H_+^R|^2 + |H_-^R|^2 + |H_0|^2 \ , \tag{10}$$

where the L (R) refer to left- (right-) handed leptons and the subscripts $\pm$ and 0 indicate the transverse and longitudinal polarizations of the K^*. When the heavy quark relations (8) are imposed, the helicity amplitudes depend only on the semileptonic form factors f, g, and a_+. The transverse helicities take the form

$$\begin{aligned} H_\alpha^L = &-\left[C_7 \frac{m_b(m_B - E_* + \eta_\alpha \mathbf{k})}{q^2} + \frac{C_8 - C_9}{2}\right] \\ &\times (f + \eta_\alpha 2 m_B \mathbf{k}_g) \\ &+ \left[C_7' \frac{m_b(m_B - E_* - \eta_\alpha \mathbf{k})}{q^2} + \frac{C_8' - C_9'}{2}\right] \\ &\times (f - \eta_\alpha 2 m_B \mathbf{k}_g) \ , \end{aligned} \tag{11a}$$

$$\begin{aligned} H_\alpha^R = &-\left[C_7 \frac{m_b(m_B - E_* + \eta_\alpha \mathbf{k})}{q^2} + \frac{C_8 + C_9}{2}\right] \\ &\times (f + \eta_\alpha 2 m_B \mathbf{k}_g) \\ &+ \left[C_7' \frac{m_b(m_B - E_* - \eta_\alpha \mathbf{k})}{q^2} + \frac{C_8' + C_9'}{2}\right] \\ &\times (f - \eta_\alpha 2 m_B \mathbf{k}_g) \ , \end{aligned} \tag{11b}$$

where $\alpha = +, -$ and $\eta_\alpha = (1, -1)$. The longitudinal helicity is

$$\begin{aligned} H_0 = \frac{m_{B^2}}{2 m_{K^*}\sqrt{q^2}} \Bigg\{ &-2(C_7 - C_7') \frac{m_b}{q^2 m_B} [f(m_B E_* - m_{K^*}^2) \\ &+ 2 m_B^2 \mathbf{k}^2 g] \\ &+ \frac{C_8 - C_9 - C_8' + C_9'}{2} \left[4\mathbf{k}^2 a_+ - \frac{2E_*}{m_B} f\right] \Bigg\} \ . \end{aligned} \tag{12}$$

In (11) and (12) E_* and $\mathbf{k}$ are the energy and spatial momentum of the K^* in the B rest frame, the short-distance coefficients must be evaluated at $\mu = m_b$ and the form factors at $q^2 = m_{ll}^2$. The latter can be either the semileptonic form factors extracted from $B \to \rho l\nu$ or, by applying (9), those from $D \to K^* l\nu$. One can immediately see from (11) that there is an interesting interplay between the short-distance coefficients and the combination of form factors entering in each transverse helicity. For instance, the first term in each of (11a) and (11b) corresponds to the contributions from normal-helicity operators, whereas the second line comes from

the ones with wrong chirality. Depending on the sign η_α, some contributions will be enhanced and some suppressed by the form factors. This will lead to rather distinct signals when considering different physics scenarios at M_W or higher scales.

The angular information is most sensitive to the details of the helicity amplitudes. The forward-backward asymmetry for leptons was considered in the contexts of both inclusive [6] and exclusive [9] $b \to s l^+ l^-$ processes. Defining θ_l as the polar angle formed by the l^+ and the B meson in the l^+l^- rest frame, the double-differential decay rate has the form

$$\frac{d^2\Gamma}{dq^2 d\cos\theta_l} = \frac{G_F^2\alpha^2|V_{tb}^*V_{ts}|^2}{768\pi^5 m_B^2}\mathbf{k}q^2\{(1+\cos\theta_l)^2[|H_+^L|^2+|H_-^R|^2]+(1-\cos\theta_l)^2[|H_-^L|^2+|H_+^R|^2]+2\sin^2\theta_l|H_0|^2\}\ . \quad (13)$$

Then the forward-backward asymmetry is defined by

$$A_{\rm FB}(q^2) = \frac{\int_0^1 (d^2\Gamma/dq^2 d\cos\theta_l)dq^2 - \int_{-1}^0 (d^2\Gamma/dq^2 d\cos\theta_l)dq^2}{\int_0^1 (d^2\Gamma/dq^2 d\cos\theta_l)dq^2 + \int_{-1}^0 (d^2\Gamma/dq^2 d\cos\theta_l)dq^2} \quad (14)$$

which, making use of (13), gives

$$A_{\rm FB} = \frac{3}{4}\frac{|H_-^L|^2+|H_+^R|^2-|H_+^L|^2-|H_-^R|^2}{|H_-^L|^2+|H_+^R|^2+|H_+^L|^2+|H_+^R|^2+|H_0|^2}\ . \quad (15)$$

Alternatively, one can simply use the angular distribution. In the next section we present results for the asymmetry and the dilepton mass distributions in several theories, including the SM.

B. $B \to K l^+ l^-$

We now turn to the pseudoscalar decay mode. The hadronic matrix elements of the operators O_i and O_i', $i = 7, 8, 9$, are now

$$\langle K(k)|\bar{s}\sigma_{\mu\nu}b|B(P)\rangle = D[(P+k)_\mu(P-k)_\nu - (P+k)_\nu(P-k)_\mu]\ , \quad (16)$$

$$\langle K(k)|\bar{s}\gamma_\mu b|B(P)\rangle = f_+(P+k)_\mu + f_-(P-k)_\mu\ , \quad (17)$$

with D, and $f_\pm$ unknown functions of $q^2 = m_{ll}^2$. Using (7) one obtains

$$D = -\frac{f_+ - f_-}{2m_B}\ . \quad (18)$$

In the SU(3) limit $f_\pm$ are the $B \to \pi l\nu$ form factors. Measurements of this mode already exist [18] but are still not precise enough. On the other hand, the flavor heavy quark symmetry predicts [3]

$$(f_+ - f_-)^B(v\cdot k) = \sqrt{\frac{m_B}{m_D}}(f_+ - f_-)^D(v\cdot k)\ , \quad (19)$$

where the B and the D labels refer to the $B \to K l^+ l^-$ and $D \to K l\nu$ decays, respectively. The window in which a reliable prediction for $B \to K l^+ l^-$ can be obtained from the charm semileptonic decay data is now $4.2 < m_{ll} < 4.8$ GeV. The dilepton mass distribution takes the form

$$\frac{d\Gamma}{dq^2} = \frac{G_F^2|V_{tb}^*V_{ts}|^2\alpha^2\mathbf{k}^2}{192\pi^5}\{|(C_8+C_8')f_+ - 2Dm_b(C_7+C_7')|^2 + |(C_9+C_9')f_+|^2\}\ . \quad (20)$$

From (20) it can be seen that the chirality of the operators is not tested in this mode. It is not possible to distinguish a shift in the coefficients of the normal operator basis from a nonzero value of the "wrong" chirality operators in (3). The information of this decay could be, however, an important complement to $B \to K^* l^+ l^-$.

IV. PREDICTIONS

In this section we consider various electroweak symmetry breaking scenarios and their signals in $B \to K^{(*)} l^+ l^-$ decays. The main purpose is to illustrate the potential of these rare decays to discriminate among theories. The results presented here make use of the form factor relations (8) *and* (9). The use of the latter implies a restriction of the theoretically safe predictions to the region with $m_{ll} > 4.0$ GeV in the $B \to K^* l^+ l^-$ case. We slightly extend this region down to 3.8 GeV to cover the dilepton mass region above the Ψ' background from the indirect process $B \to K^*\Psi' \to K^* l + l^-$. For the $B \to K l^+ l^-$ case we present results for the region $4.2 < m_{ll} < 4.8$ GeV, which is allowed by the use of $D \to K l\nu$ data in (19).

A. Standard model

At the electroweak scale the only operators contributing to the $b \to s l^+ l^-$ transitions are O_7, O_8, and O_9. However, when evolved down to the b quark scale, they mix with O_1 and O_2. The coefficients at $\mu = M_W$ are [20]

$$C_7(M_W) = -\tfrac{1}{2} A(x) \ , \tag{21}$$

$$C_8(M_W) = \frac{-B(x)}{s^2\theta_w} - \frac{4s^2\theta_w - 1}{s^2\theta_w} C(x) - D(x) + \frac{4}{9} \ , \tag{22}$$

$$C_9 = \frac{B(x)}{s^2\theta_w} - \frac{C(x)}{s^2\theta_w} \ , \tag{23}$$

where $x = (m_t^2/M_W^2)$ and with

$$A(x) = \frac{x}{(x^3-1)} \left\{ \frac{2}{3}x^2 + \frac{5}{12}x - \frac{7}{12} - \frac{x(3/2x-1)}{x-1} \ln x \right\} \ , \tag{24}$$

$$B(x) = \frac{x}{4(x-1)} \left\{ \frac{1}{x-1} \ln x - 1 \right\} \ , \tag{25}$$

$$C(x) = \frac{x}{4(x-1)} \left\{ \frac{x}{2} - 3 + \frac{(3/2x^2+1)}{x-1} \ln x \right\} \ , \tag{26}$$

$$D(x) = \frac{1}{(x-1)^3} \left\{ \frac{25}{36}x^2 - \frac{19}{36}x^3 + \frac{(-x^4/6 + \frac{5}{3}x^3 - 3x^2 + \frac{16}{9}x - \frac{4}{9})}{x-1} \ln x \right\} \ . \tag{27}$$

We also need $C_1(M_W) = 0$ and $C_2(M_W) = -1$. Defining $\eta = \alpha_s(m_b)/\alpha_s(M_W)$, the evolution to m_b gives [11]

$$C_7(m_b) = \eta^{-16/23} \{ C_7(M_W) - \tfrac{58}{135}(\eta^{10/23} - 1) C_2(M_W) - \tfrac{29}{189}(\eta^{28/23} - 1) C_2(M_W) \} \ , \tag{28}$$

$$C_8(m_b) = C_8(M_W) + \frac{4\pi}{\alpha_s(M_W)} \left\{ \tfrac{4}{33}(\eta^{11/23} - 1) + \tfrac{8}{27}(1 - \eta^{-29/23}) \right\} C_2(M_W) + [C_1(m_b) + C_2(m_b)] g(m_c/m_b; q^2) \ , \tag{29}$$

where

$$C_{1,2}(m_b) = \tfrac{1}{2}[\eta^{-6/23} \mp \eta^{12/23}] C_2(M_W) \tag{30}$$

and the last term in $C_8(m_b)$ comes from the one-loop contributions of O_1 and O_2, which gives a dependence on q^2. For $q^2 > 4m_c^2$ it is given by the function

$$g(z,s) = -\left\{ \frac{4}{9} \ln z^2 - \frac{8}{27} - \frac{16}{9}\frac{z^2}{s} + \frac{2}{9}\sqrt{1 - \frac{4z^2}{s^2}} \left(2 + \frac{4z^2}{s^2}\right) \left[\ln \left| \frac{1 + \sqrt{1 - \frac{4z^2}{s^2}}}{1 - \sqrt{1 - \frac{4z^2}{s^2}}} \right| + i\pi \right] \right\} \ , \tag{31}$$

where the imaginary part arises when the charm quarks in the loop go on shell. In calculating the asymmetry and dilepton mass distribution we do not include the long-distance pieces coming from the $B \to K^* J/\psi$ plus $J/\psi \to l^+ l^-$ or the analogous process for the ψ'. The limitations from using $D \to K^* l\nu$ data keep our predictions at m_{ll} above these contributions.

We are now in the position of calculating the forward-backward asymmetry for leptons and the dilepton mass distribution in the SM. We use $m_t = 175$ GeV for the evaluation of the short-distance coefficients and we take $|V_{tb}^* V_{ts}| \approx s^2\theta_c$. As it can be seen in Fig. 2(a), the SM has a large and negative $A_{\rm FB}$. This is due to the fact that the largest helicity amplitude is $|H_+^L|$. The right-handed lepton amplitudes are negligible, mostly due to cancellations among short-distance coefficients, whereas $|H_-^L|$ is suppressed by the combination of form factors entering in (11a) with $\eta_- = 1$. The dilepton mass distribution is shown in Fig. 3(a).

B. Two-Higgs-doublet models

As a first extension of the minimal SM we consider an extension in the Higgs sector. In models with two Higgs doublets, tree-level flavor-changing neutral currents are avoided by coupling quarks of the same charge to the same Higgs doublet. One such model corresponds to all fermions getting their masses from one Higgs doublet (model I) whereas another alternative is to have the up quarks getting their masses from one scalar doublet and the down quarks from the other. The resulting couplings of the charged Higgs boson to quarks imply a new contribution to the loop in Fig. 1 by replacing the W with the charged Higgs boson. These contributions have been extensively studied in the literature [11,12]. They effectively shift the values of the short-distance coefficients C_7, C_8, and C_9 at $\mu = M_W$. In model I we have

$$C_7(M_W) = -\frac{1}{2}A(x) + \left[\left(\frac{v_1}{v_2}\right)^2 G(y) - \frac{1}{6}A(x)\right] , \quad (32)$$

whereas, in model II,

$$C_7(M_W) = -\left(\frac{1}{2}A(x) + G(y) + \frac{1}{6}\left(\frac{v_1}{v_2}\right)^2 A(x)\right) , \quad (33)$$

where

$$G(y) = \frac{y}{2(y-1)^2}\left[\frac{5}{6}y - \frac{1}{2} - \frac{y-2/3}{y-1}\ln y\right] \quad (34)$$

with $x = m_t^2/M_W^2$ and $y = m_t^2/m_h^2$. The coefficients C_8 and C_9 at the electroweak scale are identical in both models and are given by

$$C_8(M_W) = \frac{-B(x)}{s^2\theta_w} - \frac{4s^2\theta_w - 1}{s^2\theta_w}\left[C(x) - \left(\frac{v_1}{v_2}\right)\frac{x}{2}B(y)\right] - D(x) + \frac{4}{9} - \frac{v_1}{v_2}yF(y) , \quad (35)$$

$$C_9(M_W) = \frac{B(x)}{s^2\theta_w} - \frac{1}{s^2\theta_w}\left[C(x) - \left(\frac{v_1}{v_2}\right)^2\frac{x}{2}B(y)\right] \quad (36)$$

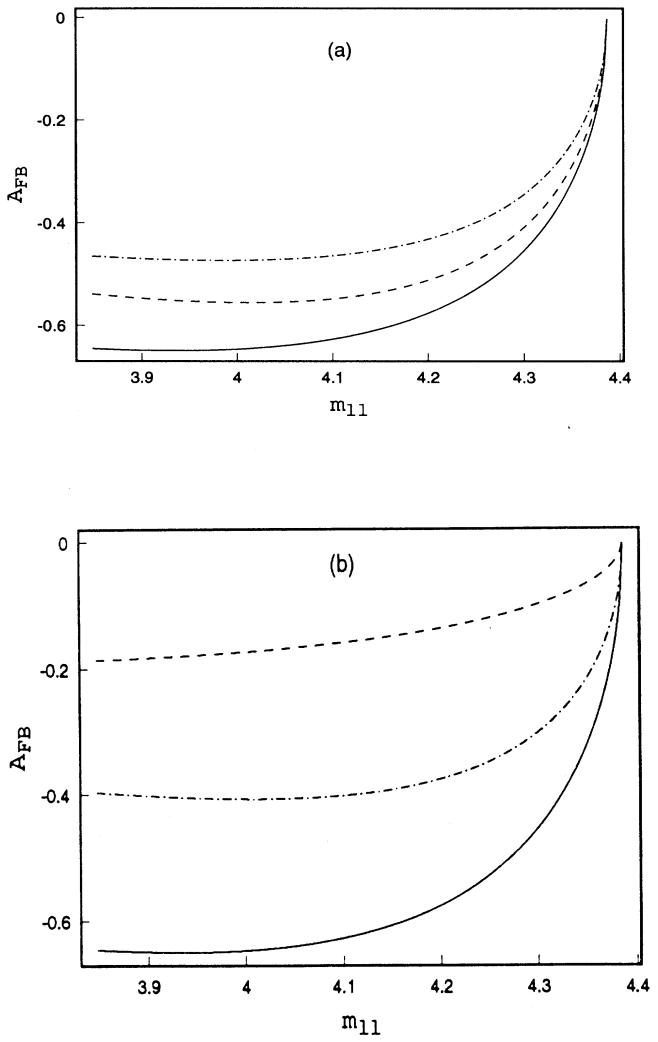

FIG. 2. Forward-backward asymmetry for leptons as a function of the dilepton mass in $B \to K^* l^+ l^-$. The solid line is the SM prediction. In (a), the dot-dashed line is the two-Higgs-doublet model I with $v_2/v_1 = 0.50$, $m_H = 100$ GeV and the dashed line is model II with $v_2/v_1 = 1$, $m_H = 300$ GeV. In (b), the dashed line is the top-color prediction for $m_{Z'} = 500$ GeV, whereas the dot-dashed line corresponds to $m_{Z'} = 1$ TeV. Both cases correspond to the square-root ansatz of Eq. (43) with a negative relative sign.

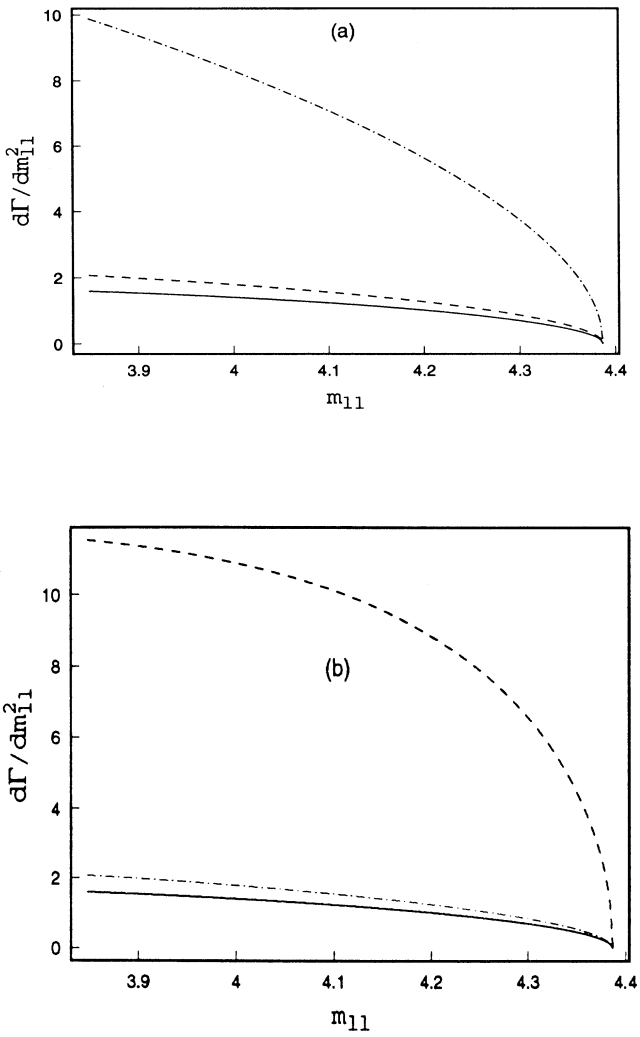

FIG. 3. Dilepton mass distributions for $B \to K^* l^+ l^-$, in units of $10^7 \times \tau_B$. The caption is the same as in Fig. 2.

with

$$F(y) = \frac{1}{(y-1)^3}\left[\frac{47}{108}y^2 - \frac{79}{108}y + \frac{19}{54} + \frac{y/3 - y^3/6 - 2/9}{y-1}\ln y\right] . \quad (37)$$

Extending the Higgs sector does not give contributions to operators outside the SM operator basis (2). The coefficients C_7', C_8', and C_9' corresponding to the operators (3) remain zero. The model is determined by the value of m_H, the charged Higgs boson mass, and v_2/v_1, the ratio of vacuum expectation values of the two-Higgs doublets. We take a representative example in each model. Model II gives and enhancement to $b \to s\gamma$ and therefore is highly constrained by experiment [1,2]. Choosing $v_2/v_1 = 1$, $m_H = 300$ GeV is at the edge of the allowed region, although the constraints are loosen if one takes into account the theoretical uncertainties related to the choices of the renormalization scale and scheme [14]. The asymmetry $A_{\rm FB}$ in this model is given by the dashed line in Fig. 2(a), whereas the dilepton mass distribution is given by the dashed line shown in Fig. 3(a).

On the other hand, in model I the coefficient C_7 governing $b \to s\gamma$ transitions may be suppressed due to cancellations, as it can be seen in (32). In fact, the extra terms may even reverse the sign of C_7. We choose as an example in this model a case in which the magnitude of C_7 is the same as in the SM but the sign is the opposite. One way of achieving this is with $v_2/v_1 = 0.50$, $m_H = 100$ GeV. Although in conflict with the current measurement of R_b at the CERN e^+e^- collider LEP [15], this choice constitutes an interesting example given that leaves the $b \to s\gamma$ unchanged, while largely modifying the values of C_8 and C_9. This translates into important changes in both the forward-backward asymmetry for leptons and the dilepton mass distribution, as can be seen in the dot-dashed lines in Figs. 2(a) and 3(a).

C. Top-color models

We now turn to a class of models that has the potential to give not only sizable shifts in the coefficients C_7, C_8, and C_9 but also can generate contributions to "wrong" chirality operators. Nonzero values of C_7', C_8', and C_9' strongly affect the pattern of helicities with respect to the SM. This can be clearly appreciated from expression (11) for the transverse helicities, where the terms containing the "wrong"-chirality coefficients are multiplied by the combination of form factors with the opposite relative sign. This implies, for instance, that H_-^L could become comparable to H_+^L, which would induce a cancellation in $A_{\rm FB}$. Right-handed helicities could also become important.

Top-color models [10] are of interest due to the fact that they give special status to the third generation through the dynamical generation of the top quark mass. The dynamics at ≈ 1 TeV is given by the gauge structure

$$\mathrm{SU(3)}_1 \times \mathrm{U(1)}_{Y_1} \times \mathrm{SU(3)}_2 \times \mathrm{U(1)}_{Y_2} \to \mathrm{SU(3)}_{\rm QCD} \times \mathrm{U(1)}_Y . \quad (38)$$

The $\mathrm{SU(3)}_1 \times \mathrm{U(1)}_{Y_1}$ couples strongly to the third generation whereas the $\mathrm{SU(3)}_2 \times \mathrm{U(1)}_{Y_2}$ is strongly coupled to the first two. The $\mathrm{SU(3)}_1 \times \mathrm{U(1)}_{Y_1}$ is assumed to be strong enough to form a chiral $\langle t\bar{t}\rangle$ condensate, but not $\langle b\bar{b}\rangle$ or $\langle \tau\bar{\tau}\rangle$ condensates, giving a large mass to the top quark. There is a residual $\mathrm{SU(3)}' \times \mathrm{U(1)}'$ which implies the existence of a massive color octet B_μ^a (top gluon) and a singlet Z_μ'. The couplings of the latter to the quarks are given by [10]

$$\mathcal{L}_{Z'} = Z_\mu' g_1 \{\tan\theta'(\tfrac{1}{3}\bar{\psi}_L\gamma_\mu\psi_L + \tfrac{4}{3}\bar{u}_R\gamma_\mu u_R - \tfrac{2}{3}\bar{d}_R\gamma_m d_R) - \cot\theta'(\tfrac{1}{3}\bar{\chi}_L\gamma_\mu\chi_L + \tfrac{4}{3}\bar{t}_R\gamma_\mu t_R - \tfrac{2}{3}\bar{b}_R\gamma_\mu b_R)\} , \quad (39)$$

where $\psi = (u,d)$, $\chi = (t,b)$, and g_1 is the $\mathrm{U(1)}_Y$ coupling. The angle θ' is small, which selects the top quark direction for condensation. The corresponding Z_μ' coupling to first- and second-generation leptons is also suppressed by $\tan\theta'$, whereas the coupling to the τ lepton is enhanced by $\cot\theta'$. After rotation to the mass eigenstates, (39) generates four-fermion interactions leading to additional contributions to the $b \to s l^+ l^-$ transitions. For $l = e, \mu$, the short-distance coefficients are independent of θ' and are given by

$$C_8 = C_8^{\rm SM} + \frac{1}{2}\kappa\frac{V_{bs}}{V_{tb}V_{ts}^*} , \quad (40a)$$

$$C_9 = C_9^{\rm SM} + \frac{1}{6}\kappa\frac{V_{bs}}{V_{tb}V_{ts}^*} , \quad (40b)$$

and, for the coefficients of (3),

$$C_8' = -\kappa\frac{W_{bs}}{V_{tb}V_{ts}^*} , \quad (41a)$$

$$C_9' = -\frac{1}{3}\kappa\frac{W_{bs}}{V_{tb}V_{ts}^*} , \quad (41b)$$

where we have defined

$$\kappa = \frac{8\pi^2 v^2}{M_{Z'}^2}\left(\frac{M_Z}{M_W}\right)^2 \quad (42)$$

and $V_{bs} = D_{bs}^{*L} D_{bb}^L$ and $W_{bs} = D_{bs}^{*R} D_{bb}^R$ are the residual nondiagonal terms in the Z' couplings after the diagonalization of the mass matrix for down-type quarks according to $D^{L\dagger} M_D D^R$. The FCNC couplings V_{bs} and W_{bs} are only fixed by a specific realization of the model. In order to make a prediction, we take them to be equal and approximately half the SM charged current equivalent V_{ts}. This corresponds to the squared-root ansatz in [10]:

$$|V_{bs}| \approx |W_{bs}| \approx \pm\tfrac{1}{2}|V_{ts}| . \quad (43)$$

Estimates of top-color contributions to other B processes, as $b \to s\gamma$ and $B^0 - \bar{B}^0$ mixing, are discussed in [10]. The results for the asymmetry are plotted in Fig. 2(b)

TABLE I. Integrated asymmetry and branching fraction in the region $m_{ll} > 3.8$ GeV in $B \to K^* l^+ l^-$. For top quark (TC) color we take into account both possible relative signs $(-/+)$ between the FCNC couplings and the corresponding CKM matrix elements.

	$a_{\rm FB}^{\rm partial}$	$10^{-6} B^{\rm partial}$
SM	-0.57	0.50
2HDM-I ($v_2/v_1 = 0.50$, $m_H = 100$ GeV)	-0.42	2.83
2HDM-II ($v_2/v_1 = 1$, $m_H = 300$ GeV)	-0.48	0.63
TC ($M_{Z'} = 500$ GeV)	$-0.138/-0.250$	4.0/5.0
TC ($M_{Z'} = 1$ TeV)	$-0.36/-0.46$	0.6/0.9

for the minus sign in (43) and for both $M_{Z'} = 500$ GeV and $M_{Z'} = 1$ TeV. In both cases, but in particular in one of them, it can be seen that the asymmetry is very different than the one obtained in the SM. The dilepton mass distributions are shown in Fig. 3(b). The effect of the Z' is striking both in the asymmetry and the dilepton mass distribution, even when looking at such a restricted region of phase space. The asymmetry becomes a more sensitive test for a much heavier Z'. For instance for $M_{Z'} = 1$ TeV the branching ratio is not much larger than in the SM, whereas the asymmetry is still significantly different. In Table I, we show the branching ratios and asymmetries corresponding to $m_{ll} > 3.8$ GeV in the cases considered above.

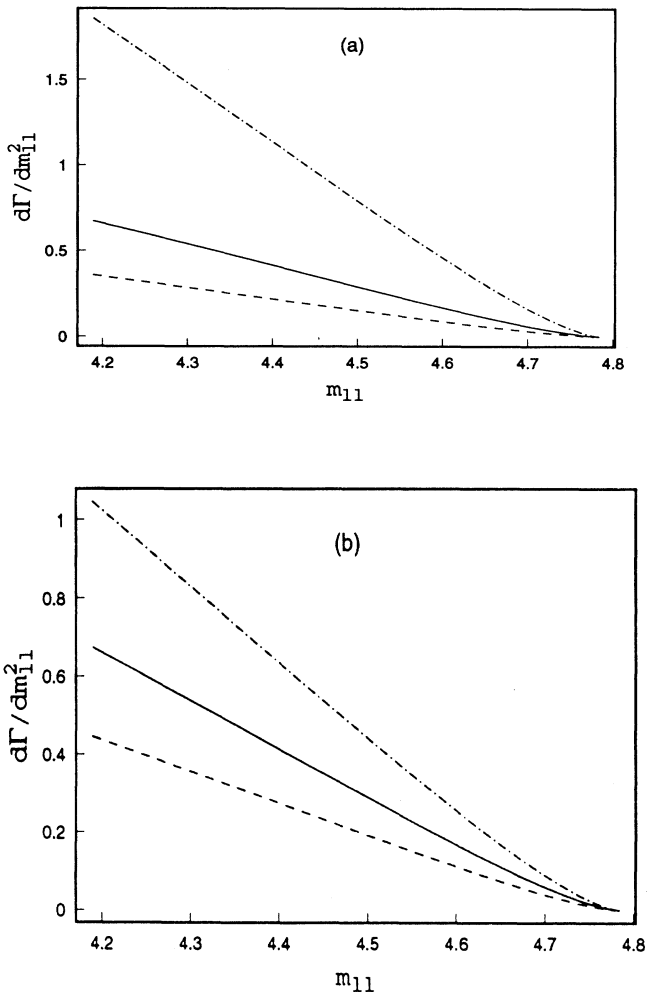

FIG. 4. Dilepton mass distributions for $B \to K l^+ l^-$, in units of $10^7 \times \tau_B$. The caption is the same as in Fig. 2.

We finally point out that top-color models as the ones considered above, that produce observable effects with $l = e$ and μ are likely to give very large effects for $l = \tau$. This is due to the fact that the four-fermion interactions induced by (39) together with the similar Lagrangian for τ leptons, are proportional to $\cot^2\theta'$. This implies large contributions to $b \to s\tau^+\tau^-$ processes like $B \to K^{(*)}\tau^+\tau^-$ and $B_s \to \tau^+\tau^-$ [21].

The results for $B \to K l^+ l^-$ can be seen in Fig. 4, where the dilepton mass distributions are plotted for the various cases considered above and in the region allowed by the use of the relations (19). It can be seen that this mode is not such a powerful test of the SM. However its observation will be an important complement to the information extracted from $B \to K^* l^+ l^-$. The results for this decay are summarized in Table II.

V. CONCLUSIONS

As we have seen in previous sections, the decay $B \to K^* l^+ l^-$ is a powerful test of the SM. This is true even when the present experimental situation restricts the reliable predictions of hadronic matrix elements to the region with $m_{ll}^2 > m_{\Psi'}^2$. The angular information is likely to be an extremely useful tool given its sensitivity to changes in the short distance coefficients in (1). The forward-backward asymmetry $A_{\rm FB}$ is very large and negative in the SM, as it can be seen in Fig. 2(a) and in Table I. This is caused by an accidental partial cancellation in the short-distance factor that makes the helicity H_+^L to be significantly larger than all the others, causing a large negative value in (15).

The two-Higgs-doublet scenarios we discussed in Sec. IV are a good example of the type of modifications to be expected in the asymmetry and the dilepton mass distribution. Model I is an example of new physics that gives the same $b \to s\gamma$ rate as the SM, but will have very different branching ratios and angular distributions in $b \to s l^+ l^-$. This can be seen in Figs. 2(a), 3(a), and 4(a).

We have also considered the effects of top-color models

TABLE II. Integrated branching fraction in the region $m_{ll} > 4.2$ GeV in $B \to K l^+ l^-$. For TC we take into account both possible relative signs $(-/+)$ between the FCNC couplings and the corresponding CKM matrix elements.

	$10^{-7} B^{\text{partial}}$
SM	1.6
2 HDM-I ($v_2/v_1 = 0.50$, $m_H = 100$ GeV)	4.5
2 HDM-II ($v_2/v_1 = 1$, $m_H = 300$ GeV)	0.9
TC ($M_{Z'} = 500$ GeV)	1.1/2.5
TC ($M_{Z'} = 1$ TeV)	0.6/1.0

[10], as an example of a theory that gives contributions to "wrong" chirality operators. The $b \to s l^+ l^-$ decays are the first low-energy data that could be strongly affected by the phenomenology of these models, which are also expected to produce important effects on top and bottom production [22] as well as on $\Gamma(Z \to b\bar{b})$ [23]. We have seen in Sec. IV that a 500-GeV color-singlet boson strongly coupled to the third generation gives large deviations from the SM in both the asymmetry and the dilepton mass distribution, as long as the neutral mixing induced is chosen to be of the same order as the corresponding Cabibbo-Kobayashi-Maskawa (CKM) matrix element as in (43). The asymmetry [Fig. 2(b), dashed line] is largely reduced with respect to the SM value. This is due not only to shifts in the coefficients C_8 and C_9 which upset the cancellation taking place in the SM, but also due to nonzero values of C_8' and C_9', the coefficients of the "wrong" chirality operators O_8' and O_9' in (3). The latter implies important contributions to helicity amplitudes that were largely suppressed in the SM. The sensitivity of the angular information to nonzero values of these coefficients is illustrated in the case $m_{Z'} = 1$ TeV. There, the dilepton mass distribution [Fig. 3(b), dot-dashed line] is not very different from the SM prediction. However, the asymmetry is still substantially smaller, as can be appreciated from Fig. 2(b). The information in the figures is presented in a different form in Tables I and II.

Although it is true that reliable predictions for the hadronic matrix elements are presently limited to large dilepton masses, this might not be such an important limitation regarding the quality of the angular information. The availability of $B \to \rho l \nu$ data will allow SM tests for all dilepton masses in $B \to K^* l^+ l^-$. However, the distinctive features of the angular information are likely to disappear or not be so important for smaller m_{ll}^2. For instance, the SM asymmetry will not be so large for smaller m_{ll}^2 due to the absence of a near cancellation in some of the short-distance factors in (11). This suggests that concentrating on the region of large m_{ll}^2 is not just convenient because of the lack of information from $B \to \rho l \nu$, but also because the angular information is most discriminating there. The pseudoscalar mode $B \to K l^+ l^-$ is not as rich in information as $B \to K^* l^+ l^-$ is, but it can be an important complement to it. For instance, in some extensions of the SM the $B \to K l^+ l^-$ is smaller than in the SM whereas in others is larger. This is clearly illustrated in the examples considered above and is shown in Fig. 4 and in Table II.

In the near future experiments in both hadron and e^+e^- colliders will have sensitivity to branching fractions as the ones in Tables I and II. The current upper limit corresponds to a partial branching fraction in the region we have considered, of approximately $(1\text{–}2)\times 10^{-5}$ [4,5] for the $B \to K^* l^+ l^-$ mode. Therefore, experimental information is about to start constraining new physics models and soon will be at the level of the SM predictions. The reconstruction of the dilepton asymmetries will then be an important probe into the physics of the electroweak symmetry-breaking scale.

ACKNOWLEDGMENTS

The author thanks Marcia Begalli, Gerhard Buchalla, Fritz De Jongh, and Chris Hill for useful suggestions and comments. This work was supported by the U.S. Department of Energy.

[1] CLEO Collaboration, M. S. Alam *et al.*, Phys. Rev. Lett. **74**, 2885 (1995).
[2] S. Bertolini, F. Borzumati, A. Masiero, and G. Ridolfi, Nucl. Phys. **B353**, 591 (1991); V. Barger, M. S. Berger, and R. J. N. Phillips, Phys. Rev. Lett. **70**, 1368 (1993); J. Hewett, Phys. Rev. Lett. **70**, 1045 (1993); also in *Spin Structure and High Energy Processes*, Proceedings of the 21st SLAC Summer Institute, Stanford, California, 1993, edited by L. De Porrel and C. Dunwoodie (SLAC Report No. 444, Stanford, 1994).
[3] N. Isgur and M. B. Wise, Phys. Rev. D **42**, 2388 (1990).
[4] CLEO Collaboration, P. Avery *et al.*, Phys. Lett. B **223**, 470 (1989); CLEO Collaboration, R. Balest *et al.*, in *Proceedings of the 27th International Conference on High Energy Physics*, Glasgow, Scotland, 1994, edited by P. J. Bussey and I. G. Knowles (IOP, London, 1995).
[5] CDF Collaboration, C. Anway-Wiese, in *The Albuquerque Meeting*, Meeting of the Division of Particles and Fields of the APS, Albuquerque, New Mexico, 1994, edited by S. Seidel (World Scientific, Singapore, 1995).
[6] A. Ali, T. Mannel, and T. Morozumi, Phys. Lett. B **273**, 505 (1991); A. Ali, G. F. Giudice, and T. Mannel, Z. Phys. C **67**, 417 (1995).
[7] G. Baillie, Z. Phys. C **61**, 667 (1994).
[8] C. Greub, A. Ioannissian, and D. Wyler, Phys. Lett. B **346**, 149 (1995).
[9] D. Liu, Phys. Lett. B **346**, 355 (1995).
[10] C. T. Hill, Phys. Lett. B **345**, 483 (1995).
[11] B. Grinstein, M. J. Savage, and M. B. Wise, Nucl. Phys. **B319**, 271 (1989).
[12] B. Grinstein, R. Springer, and M. B. Wise, Nucl. Phys. **B339**, 269 (1990).
[13] A. J. Buras, M. Misiak, M. Münz, and S. Pokorski, Nucl. Phys. **B424**, 374 (1994); M. Ciuchini, E. Franco, G. Mar-

tinelli, L. Reina, and L. Silvestrini, Phys. Lett. B **316**, 127 (1993); M. Ciuchini, E. Franco, L. Reina, and L. Silvestrini, Nucl. Phys. **B421**, 41 (1994).
[14] A. J. Buras and M. Münz, Phys. Rev. D **52**, 186 (1995).
[15] LEP Electroweak Working Group, P. Antilogus *et al.*, "A Combination of Preliminary LEP Electroweak Results for the 1995 Summer Conferences," Report No. DELPHI 95-137PHYS-562 (unpublished).
[16] A. Falk, M. Luke, and M. Savage, Phys. Rev. D **49**, 3367 (1994).
[17] G. Burdman and J. F. Donoghue, Phys. Lett. B **270**, 55 (1991).
[18] L. Gibbons, in Electroweak Interactions and Unified Theories, Proceedings of the XXXth Rencontres de Moriond, Les Arcs, France, 1995 (unpublished).
[19] R. J. Morrison and J. D. Richman, in Particle Data Group, L. Montanet *et al.*, Phys. Rev. D **50**, 1173 (1994), p. 1565.
[20] T. Inami and C. S. Lim, Prog. Theor. Phys. **65**, 297 (1981).
[21] G. Buchalla, G. Burdman, C. T. Hill, and D. Kominis, "GIM Violation and New Dynamics of the Third Generation," Report No. Fermilab-Pub-95/322-T (unpublished).
[22] C. T. Hill and S. J. Parke, Phys. Rev. D **49**, 4454 (1994).
[23] C. T. Hill and X. Zhang, Phys. Rev. D **51**, 3563 (1995).